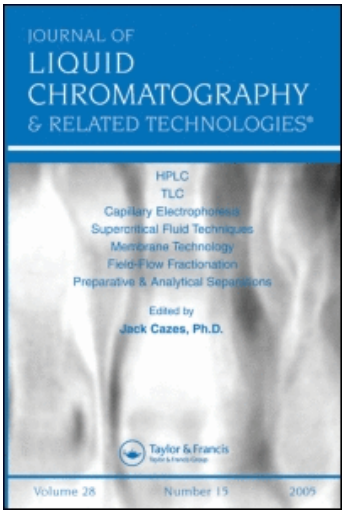

Journal of Liquid Chromatography & Related Technologies

Publication details, including instructions for authors and subscription information:
http://www.informaworld.com/smpp/title~content=t713597273

Continuous Viscometric Detection in Size Exclusion Chromatography

James Lesec[a]; Didier Lecacheux[b]; Gilles Marot[c]
[a] Laboratoire de Physico-Chimie, Macromoleculaire Universite Pierre et Marie Curie Unite Associee au CNRS n°278 E.S.P.C.I., Paris, Cedex, France [b] S.N.E.A.(P.) Groupe de Recherches de LACQ B.P., Artix, France [c] ATOCHEM, Groupe Elf Aquitaine Cerdato, Serquigny, France

To cite this Article Lesec, James , Lecacheux, Didier and Marot, Gilles(1988) 'Continuous Viscometric Detection in Size Exclusion Chromatography', Journal of Liquid Chromatography & Related Technologies, 11: 12, 2571 — 2591
To link to this Article: DOI: 10.1080/01483918808076747
URL: http://dx.doi.org/10.1080/01483918808076747

JOURNAL OF LIQUID CHROMATOGRAPHY,11(12),2571-2591(1988)

CONTINUOUS VISCOMETRIC DETECTION IN SIZE EXCLUSION CHROMATOGRAPHY

JAMES LESEC[1], DIDIER LECACHEUX[2], AND GILLES MAROT[3]

[1]*Laboratoire de Physico-Chimie Macromoleculaire*
Universite Pierre et Marie Curie
Unite Associee au CNRS n°278
E.S.P.C.I. - 10, rue Vauquelin
75231 Paris Cedex 05, France
[2]*S.N.E.A.(P.) Groupe de Recherches de LACQ*
B.P. 34 - 64170 ARTIX, France
[3]*ATOCHEM,Groupe Elf Aquitaine*
Cerdato 27470 Serquigny, France

ABSTRACT

Continuous viscometric detection is based on the measurement of pressure drop in an on-line small capillary tube in which chromatographic eluents flow at constant flow rate. This detector is always coupled with a concentration detector (usually refractometer) and located before it to avoid back pressure in the refractometer. In order to obtain reliable information for polymer samples, it is generally necessary to connect these two detectors to a computer which performs data acquisition and treatment.

First,we discuss the problem of shape, geometry and dimensions of the viscometer. The typical characteristics are the result of a compromise between contradictory targets, mainly small internal volume, low shear rate and low pressure drop. It is shown that Poiseuille's laminar flow is only obtained when coiling radius of the measurement tube is greater than 6 cm, which is not the case inside the refractometer. Accordingly, two pressure transducers are necessary to eliminate pressure drop data coming from refractometer.

---

* *To whom correspondence should be adressed.*

Paper presented at the GPC Symposium 87 - Chicago - May 1987

In a second part, we show how to extract information from pressure variation data. By using concentration data, pure solvent pressure and sample pressure it is possible to calculate intrinsic viscosity extrapolated to zero concentration at each point of the chromatogram. By comparison with intrinsic viscosity of the polymer used for calibration, a correction of hydrodynamic volume according to Benoit's universal calibration leads to absolute molecular weights.

In addition, for a linear polymer, the knowledge of log $[\eta]$ versus log M leads to the determination of Mark-Houwink relationship coefficients. For branched polymers, viscosity laws are curved and the comparison between the linear law corresponding to the linear equivalent polymer and the experimental law allows the determination of the g' branching parameter distribution.

INTRODUCTION

Benoit's universal calibration (1) requires viscosity measurements for the absolute determination of the distribution curve and average molecular weights of polymers. In Modern Size Exclusion Chromatography, classical viscometers (2,3) which gave excellent results some years ago, even at high temperature for the characterization of polyolefins (4), cannot be used because of their excessive volume of measurement. Only the on-line continuous viscometer, first described by Ouano (5) and based on the continuous measurement of the effluent pressure drop through a capillary tube, is convenient (6). After preliminary trials (7-8), the coupling of high speed GPC with the continuous viscometer was performed at high temperature for the determination of long-chain branching in polyethylene (9) and ethylene-vinyl acetate copolymers (10). A complete study of the viscometer (11) led the Société Nationale Elf Aquitaine to patent the resultant device. We will discuss, here, the performance and the functional parameters of this continuous viscometer.

CONTINUOUS VISCOMETER BACKGROUND

Principle

The principle of continuous viscometer detection is based upon the continuous measurement of the pressure drop through a small diameter capillary tube through which chromatographic eluents flow. When experimental conditions are well-chosen, corresponding to laminar flow, the pressure drop P is given by the Poiseuille relationship :

$$P = \frac{8}{\pi} \cdot \frac{l}{r^4} \cdot \eta \cdot Q$$

where η is the absolute viscosity of eluents, Q the flow rate and l and r the length and the radius of the measurement capillary tube respectively .

As viscometric data generally require concentration data to receive a complete interpretation, the viscometer is usually coupled with a concentration

detector, generally the differential refractometer. This detector cannot withstand any overpressure at its outlet because of the great fragility of the measurement cell; accordingly, the viscometer can only be inserted between columns and refractometer, as shown in figure 1.

Functional parameters

In addition to the pressure drop value, several parameters characterize viscometer behaviour.

- the shear rate G given by : $G = \frac{4}{\pi} \cdot \frac{Q}{r^3}$
- the internal volume V given by : $V = \pi \cdot r^2 l$
- the Reynolds number R given by : $R = \frac{2}{\pi} \cdot \frac{\rho}{\eta} \cdot \frac{Q}{r}$

where ρ is the density of the eluent. These parameters will be discussed later.

When looking at Poiseuille's equation, it appears that, for a given capillary tube, the resulting back pressure is only dependent upon flow rate and viscosity. At constant flow rate, pressure variations describe viscosity variations; conversely, when the eluent viscosity is constant, the viscometer measures the flow rate. That meens that the viscometer is simultaneously a flowmeter. This function has already been described (8) and we will discuss, later, its incidence on the chromatographic equipment.

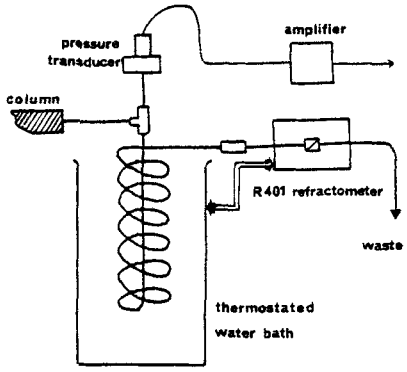

FIGURE 1 : Scheme of the continuous viscometer from (7,8).

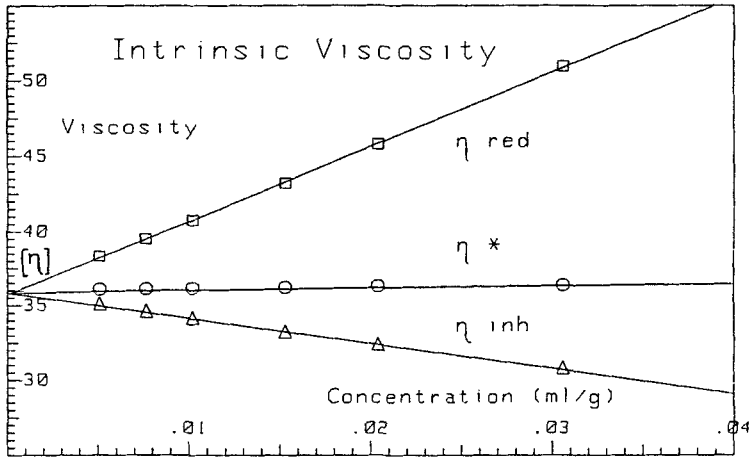

FIGURE 2 : Variations of the different viscosities versus concentration

Intrinsic viscosity calculation

Assuming that flow rate is kept constant during the chromatographic experiment, let us see how to extract intrinsic viscosity information from refractometric and viscometric data. Intrinsic viscosity $[\eta]_i$ is the extrapolated value of inherent viscosity $\eta_{i\ inh}$ and reduced viscosity $\eta_{i\ red}$ at zero concentration :

$$[\eta]_i \text{ limit of } \eta_{i\ inh} = \frac{1}{C_i} \cdot \text{Log} \frac{P_i}{P_0}$$

$$[\eta]_i \text{ limit of } \eta_{i\ red} = \frac{1}{C_i} \cdot \frac{P_i - P_0}{P_0}$$

where P_i and P_0 are, respectively, the pressure drops for macromolecular solution and pure solvent, replacing η_i and η_0 in the original equations. Since detection is achieved at very low concentration conditions, using $\eta_{i\ inh}$ or $\eta_{i\ red}$ instead of $[\eta]_i$ does not introduce a significant error; but let us define a third viscosity which will be called ηt as :

$$\eta t = \left[\frac{2}{C_i} (\eta_{i\ red} - \eta_{i\ inh}) \right]^{0.5}$$

Considering the equations giving $\eta_{1\ red}$ and $\eta_{1\ inh}$:

$$\eta_{1\ red} = [\eta]_1 + k' \cdot [\eta]_1^2 . C_1$$
$$\eta_{1\ inh} = [\eta]_1 - k'' \cdot [\eta]_1^2 . C_1$$

where k' and k'' are the Huggins and Kramer constants and replacing $\eta_{1\ red}$ and $\eta_{1\ inh}$ by their expressions, it becomes :

$$\eta_1 = [\eta]_1 \cdot [2(k' + k'')]^{0.5}$$

As in usual conditions $k' + k'' = 0.5$, we see that η_1 is identical to intrinsic viscosity, as shown in figure 2 :

$$\eta_1 \equiv [\eta]_1$$

This expression will be used in all our calculations.

THE CURVATURE EFFECT

Effect of coiling

In addition to previously described functional parameters, it appeared, during our study (11-12) that the curvature of the measurement capillary tube was an essential parameter influencing dramatically the viscometer performances. As the capillary tube is usually 2 ou 3 meter long, it seems convenient to coil it in order to insert it within a water bath or in an oven. Our first trials were run under these conditions (7-8). We have represented in figure 3 the viscometer responses of a linear capillary and a capillary coiled with a 0.8 cm radius. It appears that capillary coiling introduces an excess of pressure for high flow rates giving a deviation from Poiseuille's law. This effect was already described (13-14) and it can be explained in terms of turbulence and viscous friction. When viscosity increases, for example by dissolving a high molecular weight polymer, the effect decreases (figure 4).

Pressure/flow law can thus be represented by a 2nd degree polynomial :

$$P = k \cdot Q \cdot (1 + \alpha Q)$$

where α is the parameter representing the deviation from the Poiseuille law. From our experiments, the α parameter varies in the opposite way of the absolute viscosity η and the radius of coiling R :

$$\alpha = K \cdot \frac{1}{\eta . R}$$

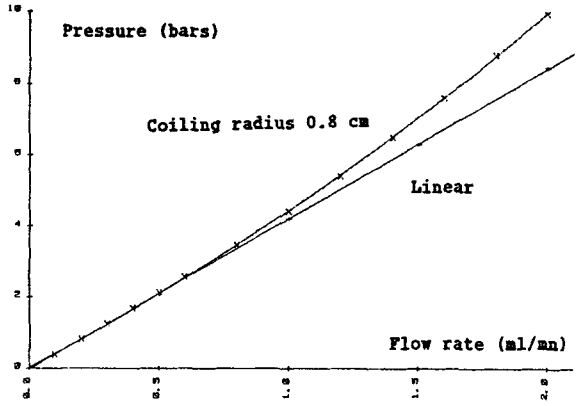

FIGURE 3 : Effect of the capillary tube curvature upon the pressure response of viscometer. Solvent : THF - Viscometer : l = 3 m r = 0.11 mm.

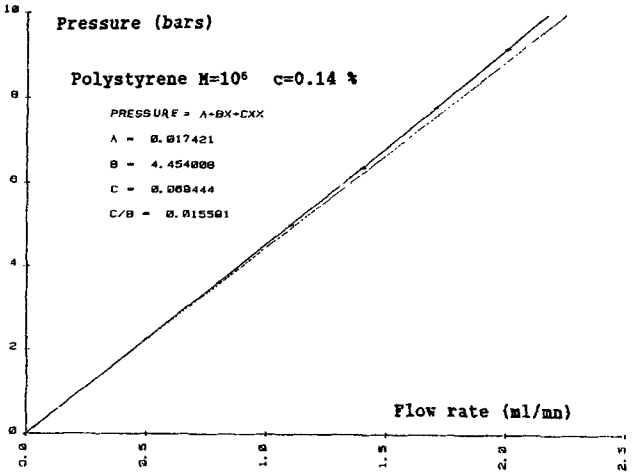

FIGURE 4 : Effect of the capillary tube curvature upon the pressure response of viscometer. Solvent : THF with polystyrene 10^6MW at a concentration of 0.14 % - viscometer : l = 3 m r = 0.11 mm R = 0.8 cm.

We have represented in figure 5, the variations of the curvature parameter a versus the radius of coiling R for THF at 30°C in a 3 meter long viscometer (0.11mm internal radius). The conclusion is that coiling smaller than 6cm introduces a dramatic deviation from Poiseuille law, above this value the effect seems negligible. In conclusion, the viscometer capillary tube can be coiled but only with a radius greater than 6cm (11-12).

Influence of coiling on viscosity determination

In order to check this coiling effect, we ran viscosity measurements on different polymers with various molecular weights with an Ubbelohde viscometer (providing the $[\eta]_0$ value) and with a continuous viscometer, 3 meter long, 9/1000" I.D. at a flow rate of 2ml/mn of THF (providing the $[\eta]_G$ value). All the results are reported in Table I.

A systematic difference is observed between absolute intrinsic viscosities and those obtained by the continuous viscometer, the average ratio of $[\eta]_G/[\eta]_0$ being approximately 0.78.

According to our previous calculations, we can write the expressions of the experimental pressure drops :

$$P_0' = P_0 \ (1 + \alpha_0 \ Q)$$
$$P_1' = P_1 \ (1 + \alpha_1 \ Q)$$

Where P and P' are respectively the theoretical and experimental pressures (index 0 refers to pure solvent and index 1 to polymer solution). The experimental inherent viscosity η'_{inh} can thus be writen as :

$$\eta'_{inh} = \frac{1}{C} \text{Log} \frac{P_1'}{P_0'} = \frac{1}{C} \text{Log} \left(\frac{P_1 \ (1 + \alpha_1 \ Q)}{P_0 \ (1 + \alpha_0 \ Q)} \right)$$

or

$$\eta'_{inh} = \eta_{inh} - \frac{1}{C} (\alpha_0 - \alpha_1) \ Q$$

It comes :
$$\alpha_0 - \alpha_1 = \frac{1}{Q} \cdot C \cdot \eta_{inh} \left(1 - \frac{\eta'_{inh}}{\eta_{inh}}\right)$$

The same calculation can be performed on the reduced viscosity but in order to simplify the demonstration, let us consider that the inherent viscosity is almost like intrinsic viscosity. We can write :

$$\alpha_0 - \alpha_1 = \frac{1}{Q} \cdot C \cdot [\eta] \cdot \left(1 - \frac{[\eta]_G}{[\eta]_0}\right)$$

TABLE I

Comparison between $[\eta]_o$ determined by Ubbelohde viscometry and $[\eta]_G$ measured by the continuous viscometer for various polymers.

Polymers	Origin	Label	$\bar{M}_w$	I	$[\eta]_o$	$[\eta]_G$	$[\eta]_G/[\eta]_o$
Polystyrene	Waters	35 000	38 000	1.02	27.5	21.8	0.79
	Waters	110 000	112 800	1.02	56.5	42.4	0.75
	SNEA	PSL 134	189 600	1.71	74.9	61.3	0.81
	Waters	200 000	233 000	1.06	94.7	70.6	0.75
	SNEA	BASF168N	272 400	1.90	101.2	82.2	0.81
	Strasbourg	PS 7	423 400	1.05	148.2	111.1	0.75
	Waters	650 000	620 200	1.08	200	147.5	0.74
	Strasbourg	PS 8	1030 000	1.15	268	205	0.75
	Waters	2.7 M	2340 000	1.90	462	308	0.67
	Waters	3.7 M	3350 000	1.63	605	360	0.60
Polyoxyethylene	Touzart	4 000	4 900	1.03	9.30	7.1	0.76
	Fluka	6 000	10 300	1.04	15.35	11.5	0.75
	Fluka	10 000	16 100	1.04	22.9	17.75	0.77
	Fluka	20 000	22 500	1.03	29.2	22.3	0.76
	Serva	40 000	37 400	1.06	44	33.3	0.76
Polytetra-hydrofuran	Interchim	10 000	10 680	1.13	21.2	16.1	0.76
	Interchim	30 000	35 200	1.07	61.7	44.8	0.73
	Interchim	100 000	109 000	1.09	188	140.4	0.75
	Interchim	300 000	266 800	1.64	335	266	0.80
Nitrocellulose	SNPE	CP2 P17	120 000	2.7	390	309	0.79
	SNPE	CP1 D9	59 000	2	232	173	0.75
Polymethyl-methacrylate	Interchim	P601830	68 500	1.04	28.4	23.5	0.83
Polycarbonate	Interchim	P596760	22 000	1.7	44.2	35.8	0.81

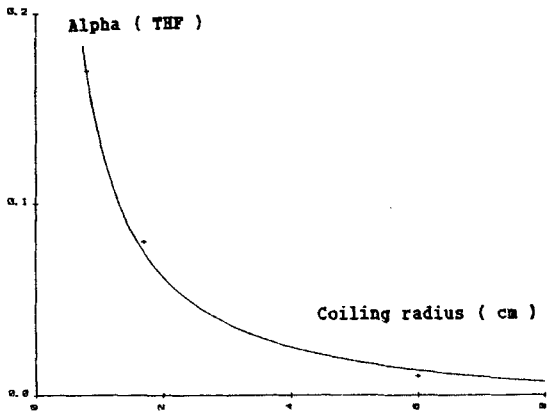

FIGURE 5 : Variations of the curvature parameter α as a function of the radius of coiling R.

TABLE II

Curvature parameters α for THF and various polymers at different concentrations. Coiling radius R = 1.8 cm

Sample	Concentration	b	c	$\alpha = \frac{c}{b}$
T.H.F.	-	3.091	0.2238	0.0724
PolyTHF 10 000	0.433 %	3.354	0.2006	0.0598
PolyTHF 30 000	0.3876 %	3.921	0.1427	0.0364
PolyTHF 100 000	0.208 %	4.439	0.1448	0.0326
PolyTHF 300 000	0.191 %	5.635	0.0476	0.0084
PS 100 000	0.556 %	4.074	0.1503	0.0369
PS 400 000	0.1824 %	3.994	0.1408	0.0353
PS 1 000 000	0.14 %	4.454	0.0694	0.0156

We measured the curvature parameter a for THF and various polymers in the above described conditions (Table II) and plotted the experimental values of $\alpha_0 - \alpha_1$ versus $[\eta].C$ (figure 6). A straight line fits the experimental points leading to a slope value of 0.11. As the flow rate was 2 ml/mn, it comes that :

$$\frac{[\eta]_c}{[\eta]_0} \simeq 0.78$$

In conclusion, the coiling of the measurement capillary tube creates a curvature of Poiseuille law depending on flow rate and absolute viscosity of eluent, leading to a systematic error in the determination of the intrinsic viscosity. Considering the Mark-Houwink relationship :

$$[\eta] = k \cdot M_v^a$$

under given conditions, the ratio between experimental and real intrinsic viscosity is found to be a constant that leads to a correct "a" exponent but a wrong K value (figure 7). This explains the discrepancy of the Mark-Houwink coefficients K previously published (8).

OPTIMIZATION OF THE VISCOMETER

Viscometer design

From these former results, it becomes obvious that the measurement capillary tube must not be coiled with a radius smaller than 6cm. We have thus to take into account that, when using a viscometer as described in figure 1, the pressure measured by the transducer is the summation of the pressure drop in the capillary tube and in the refractometer. As usual, refractometers have a long inlet tubing as heat exchanger (several inches of 9/1000" I.D. tube) which is very coiled, we can be sure that pressure drop in the refractometer does not obey Poiseuille's law.

In order to obtain a viscometer with a perfect pressure/flow law, it is necessary to isolate the refractometer pressure drop by adding to the assembly a second pressure transducer (9-12) as shown in figure 8. The first transducer measures pressure P_1 relative to the viscometer and the refractometer whereas the second one measures back pressure P_2 in refractometer. Both are curved but their difference $\Delta P = P_1 - P_2$ is a perfect straight line (figure 9).

Viscometer geometrical parameters

The viscometer geometry is defined by three parameters : l, r and R which are, respectively, the length, the internal radius and the coiling radius

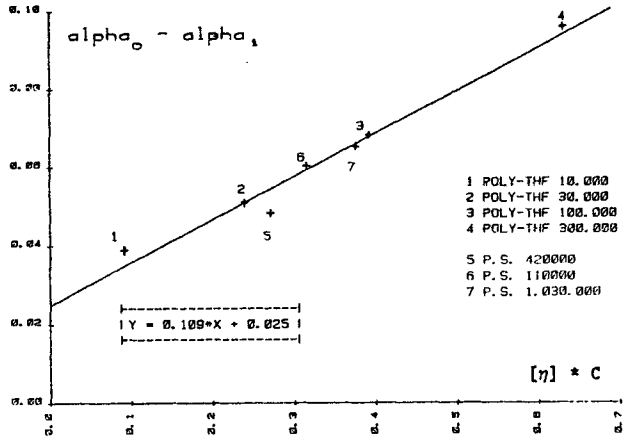

FIGURE 6 : Variation of α_o - α_1 versus [η].C for various polymers of different molecular weights.

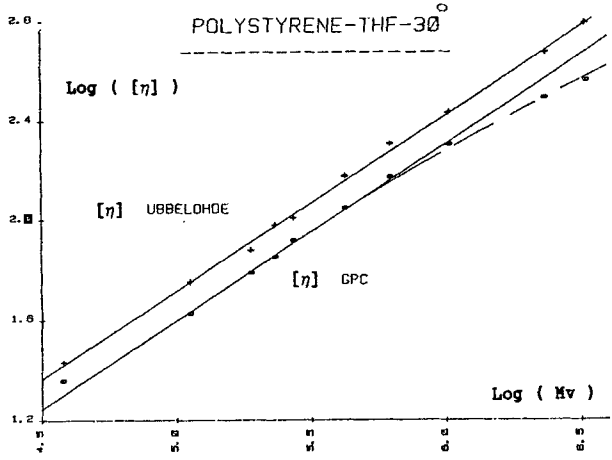

FIGURE 7 : Comparison of viscosity laws obtained by Ubbelohde viscometry and through a continuous viscometer at a flow rate of 2 ml/mn.

of the measurement capillary tube. For a given solvent at a given temperature, they determine four different functional parameters ΔP, G, V and Re which are, respectively, the pressure drop, the shear rate, the internal volume and the Reynolds number. Three of them (ΔP, G, Re) require the largest possible radius, r. Conversely, volume V is optimum when the radius is the smallest possible. Accordingly, the best value of r will be a compromise. In addition, as the refractometer itself has a non-negligible pressure drop P_2, P_1 must be something like twice the P_2 value in order to obtain a ΔP value without any loss of information. Our conclusion is that the capillary tube must have a maximum internal radius of about 0.2 mm with a length of 3 meters. Our first viscometers were based upon classical stainless steel capillary tubes (9/1000" I.D.) (9-12) but we have now adopted a Teflon capillary tube with 0.3 mm I.D. which requires special fittings (teflon/stainless steel OMNIFIT fittings) to be connected within the chromatographic circuit (15-16). We summarize, in table III, the different functional parameters of several viscometers used with THF at 30°C. The usual flow rate is 1 ml/mn.

Influence of shear rate

For the above reasons, it seems difficult, in actual conditions, that the shear rate in viscometer could reach a smaller value than 5 000 s^{-1}, which is significantly different of the classical Ubbelohde viscosity measurement conditions (1 500-2 000 s^{-1}). For high molecular weight polymers, we can expect a non-newtonian behaviour, leading to an underestimated value of viscosity. This effect is shown in figure 7. Under drastic conditions (flow rate 2ml/mn and shear rate around 20 000 s^{-1}) the deviation from the polystyrene linear law occurs for a molecular weight greater than 1 000 000. In our actual conditions (teflon viscometer with a shear rate of 5 000 s^{-1}), we can assume that deviation appears for a higher molecular weight value, but however, it is obvious that for very high molecular weight samples, especially when polydispersity is large, the viscometer response is distorted and we must be very carreful before interpreting results. In this particular case, we could imagine a special viscometer with a greater internal radius and a much lower shear rate, but which will be unable to operate with usual polymers.

Influence of flow rate

As demonstrated in the first section, the viscometer is a very accurate flowmeter; for this reason it must receive eluent from the column set with an extremely constant flow rate. Two types of variations can occur : long-time variations due to flow rate changes at the outlet of the pump and short time variations in relation with the alternate pumping principle. We mainly checked the M 6000 A solvent delivery system, installed in the Waters 150C

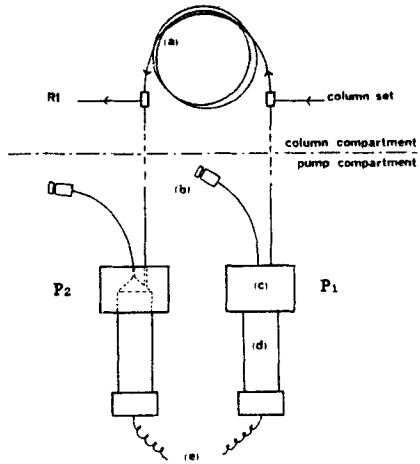

FIGURE 8 : Scheme of the continuous viscometer with two pressure transducers. (a) capillary tube. (b) purge. (c) transducer holder. (d) pressure transducers. (e) electronic units.

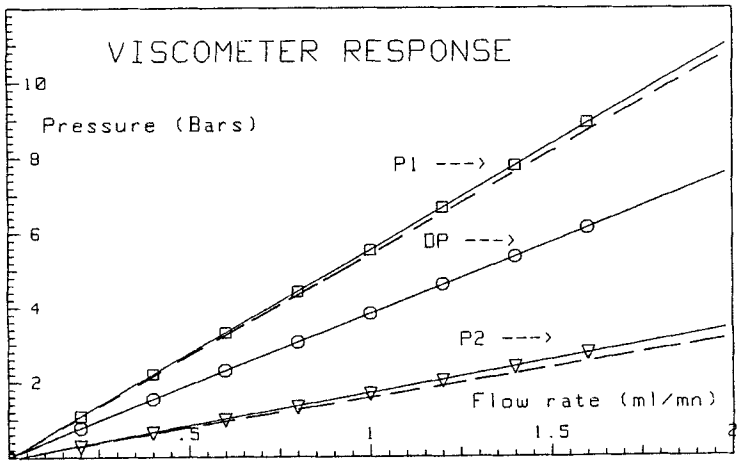

FIGURE 9 : Variations of P_1, P_2 and ΔP versus flow rate for the double transducer viscometer. THF 30°C. Viscometer l = 3 m, 9/1000" I.D.

TABLE III

Functional parameters for viscometers built with different capillary tubes.

	Stainless steel (9/1000" I.D.)			Teflon tubing	
	experim.	theoret.	used in ref.9-12	theoret.	experim.
r (mm)	0.11	0.114	0.13	0.15	0.16
ΔP (bar)	3.8	3.3	1.94	1.1	0.93
G (s^{-1})	16 000	14 300	9 700	6 200	5 100
V (μl)	110	120	160	210	240
R_e	200	190	167	145	136

TABLE IV

Comparison between apparent and absolute molecular weights for NBS 706 and DOW 1683 analyzed through a polystyrene calibration

	NBS 706		DOW 1683	
	apparent	absolute	apparent	absolute
$\bar{M}_n$	109 700	108 300	104 200	104 500
$\bar{M}_v$	249 800	248 000	223 400	222 800
$\bar{M}_w$	269 300	267 500	244 600	244 400
α	0.706	0.706	0.707	0.706
Log K	- 1.844	- 1.84	- 1.849	- 1.838
$[\eta]$	93.1	93.1	85.6	85.6
Calibration from PS Standard α = 0.706 Log K = - 1.847				

chromatograph. We were pleased to observe a negligible drift of the viscometer baseline. When the pump is in perfect running condition, the long-time variation is smaller than 1 µl/mn over 24 hours, which is excellent. Conversely, short time variations are very important. For example, at a flow rate of 1 ml/mn with a viscometer having the baseline at 1 bar, the pressure variation for a classical polymer peak is about 20 mbars which is equivalent to a flow rate variation of 20 µl/mn. In order to have a good signal/noise ratio we can consider that the baseline noise must not exceed 0.2 µl/mn. To obtain such a flow rate stability, it is necessary to reduce the pump noise by inserting between the pump and the injector, a pulse dampener based on Waters low pressure filters and restrictors. Generally, three couples are needed in alternate arrangement.

The consequence of such an accuracy is that every event which influences the flow rate more than 0.2 µl/mn has repercussions on the viscometer baseline leading to non-running conditions. The main origins of trouble are pump malfunction, injector problems, microleaks, plugging anywhere in the instrument chiefly in column end-fittings that causes important flow rate variations when a viscous solution passes through.

From another viewpoint, we can see that the presence of a continuous viscometer inside the chromatograph allows complete checking and troubleshooting of the instrument .When the viscometer baseline is right, the flow rate has a correct value and GPC measurements can be run under absolute conditions of accuracy, especially when data logging is achieved as a function of time.

Influence of internal volume

For the optimized viscometer, the internal volume is about 240 µl, which seems tremendously high with regard to classical detector cells (≃ 10 µl); but we must consider that its volume is 3 meters long and does not cause significant eluent remixing. The only disadvantage is that the viscosity measurement is not actually performed on only one fractionated molecule, but is the result of an averaging of viscosity values for all the molecules present inside the capillary tube at the measurement time. It has been shown (11) that this effect is negligible when viscometer volume is 20 times smaller than the total peak volume; that leads to an approximat value of 5 ml. This condition is fulfilled when using a column set composed of four columns (1 feet long, 7 mm I.D.) like Waters Ultrastyragel 10^3, 10^4, 10^5 and 10^6Å.

The other drawback of a large viscometer internal volume is that a molecule requires a non negligible time for passing from the viscometer to the refractometer. When data logging is achieved simultaneously for both detectors,

it is important to take into account, in the data treatment, the time required for a molecule to pass from one detector to the other, assuming that the viscometer is represented by a point located at its geometrical centre. A systematic study (17) led us to consider that the real volume difference is systematically greater than the geometrical difference. In any case, a shift of the viscometric peak must be achieved to extract reliable data from the viscometer-refractometer coupling.

RESULTS AND DISCUSSION

Use of universal calibration

The main purpose of the continuous viscometer-refractometer coupling is the use of Benoit's universal calibration to obtain absolute molecular weight values. As the viscometer continuously provides intrinsic viscosity information, the hydrodynamic volume correction can be achieved along the polymer distribution curve. For this purpose, it is only necessary to perform column calibration with a set of well-characterized molecular weight standards which gives, at the same time, the intrinsic viscosity of each standard. It is, thus, easy to determine the Mark-Houwink relationship coefficients K_{st} and a_{st} of the polymer used as standard. Using the calibration curve, established with standards, to convert the chromatogram into a distribution curve leads to an apparent distribution curve expressed in the standard units $M_{i\,st}$. Accordingly, the classical GPC calculation provides apparent average molecular weights. In order to obtain the absolute values M_i, it is simply necessary to write the equality of hydrodynamic volume $[\eta].M$ along the distribution curve :

$$M_i = \frac{K_{st}.M_{i\,st}^{(a_{st}+1)}}{[\eta]_{i\,exp}}$$

where $[\eta]_{i\,exp}$ are the experimental values of intrinsic viscosities. The classical GPC calculation now leads to absolute average molecular weights.

To check the method, it is useful to verify that, when running a sample with the same chemical nature as the standard, the hydrodynamic volume correction does not significantly modify the molecular weight values. We give in table IV the values obtained through a polystyrene calibration for two well-known polystyrene samples, NBS 706 and DOW 1683. The conversion is very satisfying.

Viscosity law determination

The second advantage of the viscometer is to provide directly the sample intrinsic viscosity $[\eta]$ without any need of refractometric data. In the $[\eta]$ definition :

$$[\eta] = \frac{\Sigma\, C_i\, [\eta]_i}{\Sigma\, C_i}$$

replacing, for example, $[\eta]_i$ by the reduced viscosity $\eta_{i\,red}$ leads to :

$$[\eta] = \frac{\Sigma\, (\Delta P_i - \Delta P_o)}{\Delta P_o \,.\, C}$$

This means that the knowledge of injection concentration C, viscometer baseline value ΔP_o and viscometric peak surface area $\Sigma\, (\Delta P_i - \Delta P_o)$ are all that are necessary to calculate the intrinsic viscosity.

But, when refractometric data are used, M_i and $[\eta]_i$ values can be calculated for every point of the chromatogram. For linear polymers, the plot of Log $[\eta]_i$ versus Log (M_i) is a straight line which is characterized by the Mark-Houwink a and K coefficients. Such a curve is represented in figure 10 for the NBS 1475 polyethylene sample. It demonstrates that, when the polymer has a sufficiently wide distribution curve (polydispersity higher than 2), the viscosity law parameters are obtained through only one sample injection (see table IV and table V).

We must remark that in figure 10, only experimental points (+) located between the two cursors are used to determine the viscosity law. Outside this area, the calculation of $[\eta]_i$ values is not accurate enough owing to the weak values of $\Delta P_i - \Delta P_o$ and C_i at the peak edges. Therefore, this points must be recalculated by extrapolation in order to obtain a reliable set of data for the hydrodynamic volume correction.

Long chain branching determination

Finally, the viscometric detection is well suited for long-chain branching characterization. In fact, long-chain branched polymers have a smaller radius of gyration R_{Gb} than that of the corresponding linear polymer R_{Gl} with the same molecular weight. The characteristic parameter of branching g is defined as the ratio of mean square radii of gyration :

$$g = \frac{\langle R_G^2 \rangle_b}{\langle R_G^2 \rangle_l}$$

Through viscosity measurements, another branching parameter g' is defined as the ratio of intrinsic viscosities :

$$g' = \frac{[\eta]_b}{[\eta]_l}$$

A simple relationship links g and g' :

$$g' = g^x$$

but the x exponent, varying from 0.5 to 1.5, is in a complex relation with the branching nature of the polymer. For particular polymers, the theory gives a relationship between g and the long chain branching frequency λ (9), allowing a better description of the polymer structure.

As the viscometer-refractometer coupling provides experimental intrinsic viscosities $[\eta]_i$ along the distribution, g'_i values can be calculated by comparison with values corresponding to the linear polymer :

$$g'_i = \frac{[\eta]_{i\ b}}{[\eta]_{i\ l}}$$

Figure 11 represents the viscosity law and the distribution of branching characterized by g'_i variations versus molecular weight for polyethylene NBS 1476.

This calculation requires a knowledge of the corresponding linear polymer viscosity law. But, when it is unknown, we have remarked, during our studies (9-11, 15-16), that branching usually occurs only after a limiting molecular weight, which produces a linear variation in the low molecular weight region of the viscosity law. Taking the slope in this region can provide the visocsity law of the linear polymer (16).

As an example, we give in table V the complete characterization of NBS 1475 and NBS 1476 polyethylene samples.

CONCLUSION

Viscometric detection in GPC experiments, when coupled with a concentration detector, greatly increases the analytical capabilities of this technique. First, it permits complete checking and troubleshooting of the GPC instrument, providing an excellent survey of experimental conditions and leading to analysis only under perfect conditions. From the viewpoint of calculation, it permits the absolute distribution curve and average molecular weight determination through universal calibration. In addition, viscosity information is obtained,such as intrinsic viscosity and viscosity law coefficients. Finally, long chain-branching distribution can be characterized and the different g' values calculated for branched polymers.

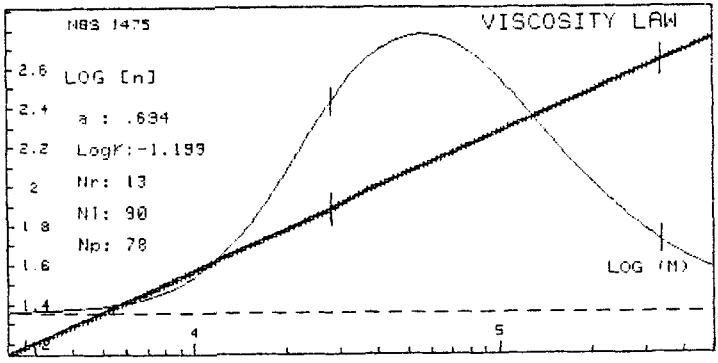

FIGURE 10 : Experimental viscosity law for NBS 1475 linear polyethylene.
(·····) viscometric trace
(——) linear viscosity law
(+++) experimental viscosity law

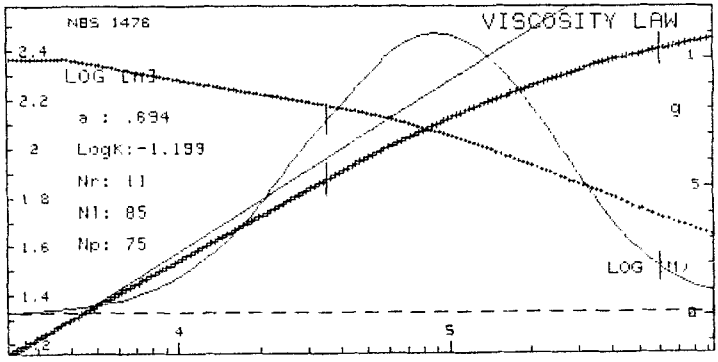

FIGURE 11 : Experimental viscosity law for NBS 1476 branched polyethylene.
(·····) viscometric trace
(——) linear viscosity law
(+++) experimental viscosity law
(+++) branching distribution g'

TABLE V

Characterization of NBS 1475 and NBS 1476 polyethylene samples.

	NBS 1475		NBS 1476	
	apparent	absolute	apparent	absolute
M_{peak}	28 690	28 990	37 330	42 270
$\bar{M}_n$	20 820	21 030	22 400	24 000
$\bar{M}_v$	43 840	43 840	50 430	63 120
$\bar{M}_w$	50 230	50 180	57 550	74 750
$\bar{M}_z$	116 100	115 700	121 000	198 300
$\bar{M}_w/\bar{M}_n$	2.41	2.39	2.57	3.11
$\bar{M}_z/\bar{M}_w$	2.31	2.31	2.1	2.65
$[\eta]$	104.6	104.6	93.3	93.3
α	.694	.694	-	-
Log K	- 1.2	- 1.2	-	-
NBS 1476 g' values				
Average	at $\bar{M}_n$	at $\bar{M}_v$	at $\bar{M}_w$	at $\bar{M}_z$
0.69	0.85	0.76	0.74	0.59

ACKNOWLEDGEMENTS

These results are a part of Didier Lecacheux thesis (11) and Gilles Marot thesis (15). Michèle Milléquant (*) ran experiments to provide the numerical data on NBS polystyrene and polyethylene samples. The authors wish to thank ATOCHEM company for financial support.

REFERENCES

1. H. Benoit, Z. Grubisic, P. Rempp, D. Dekker and J.G. Zilliox, J. Chim. Phys, 63, 1507 (1966).
H. Benoit, P. Rempp and Z. Grubisic, J. Polym. Sci., B5, 753 (1967).

2. D. Goedhart and A. Opschoor, J. Polym. Sci., A2, 8, 1227 (1970).
3. Z. Grubisic-Gallot, M. Picot, Ph. Gramain and H. Benoit, J. Applied Polym. Sci., 16, 2931 (1972).
4. D. Constantin, Eur. Polym. J., 13, 907 (1977).
5. A.C. Ouano, J. Polym. Sci., Part A1, 10, 2169 (1972).
6. A. Peyrouset and R. Prechner, Fr Patent 74-13281 (1974).
7. J. Lesec and C. Quivoron, Analusis, 4, 399 (1976).
8. L. Letot, J. Lesec anc C. Quivoron, J. of Liq. Chrom., 3(3), 427 (1980).
9. D. Lecacheux, J. Lesec and C. Quivoron, J. Applied Polym. Sci., 27, 4867 (1982).
10. D. Lecacheux, J. Lesec, C. Quivoron, R. Prechner, R. Panaras and H. Benoit, J. Applied Polym. Sci., 29, 1569 (1984).
11. D. Lecacheux, Thesis, Paris (1982).
12. D. Lecacheux, J. Lesec, R. Prechner, French Patent n°82 402 324.6 (1981). D. Lecacheux, J. Lesec, R. Prechner, US Patent n°4 478 071 - 23/10/1984.
13. H.A. Barnes and K. Walters, Nature, 216, 366 (1967).
14. R.A. Dawe, Rev. Sci. Instrum., 44, 9. 1231 (1973).
15. G. Marot, Thesis, Paris (1986).
16. G. Marot, J. Lesec, J. of Liq. Chrom., (to be published).
17. D. Lecacheux and J. Lesec, J. of Liq. Chrom., 5(12), 2227 (1982).